

Article

Liposomal Formulations of a Polyleucine–Antigen Conjugate as Therapeutic Vaccines against Cervical Cancer

Farrhana Z. Firdaus¹, Stacey Bartlett¹, Waleed M. Hussein¹, Lantian Lu¹, Quentin Wright², Wenbin Huang¹, Ummey J. Nahar¹, Jieru Yang¹, Mattaka Khongkow^{1,3}, Margaret Veitch², Prashamsa Koirala¹, Uracha R. Ruktanonchai³, Michael J. Monteiro⁴, Jazmina L. Gonzalez Cruz², Rachel J. Stephenson¹, James W. Wells², Istvan Toth^{1,5,*} and Mariusz Skwarczynski^{1,*}

¹ School of Chemistry and Molecular Biosciences, The University of Queensland, St. Lucia, QLD 4072, Australia

² Faculty of Medicine, Frazer Institute, The University of Queensland, Brisbane, QLD 4102, Australia

³ National Nanotechnology Center (NANOTEC), National Science and Technology Development Agency, 111 Thailand Science Park, Phahonyothin Rd., Khlong Luang, Pathumthani 12120, Thailand

⁴ Australian Institute for Bioengineering and Nanotechnology, The University of Queensland, Brisbane, QLD 4072, Australia

⁵ School of Pharmacy, The University of Queensland, Woolloongabba, QLD 4102, Australia

* Correspondence: i.toth@uq.edu.au (I.T.); m.skwarczynski@uq.edu.au (M.S.)

Abstract: Human papilloma virus (HPV) is responsible for all cases of cervical cancer. While prophylactic vaccines are available, the development of peptide-based vaccines as a therapeutic strategy is still under investigation. In comparison with the traditional and currently used treatment strategies of chemotherapy and surgery, vaccination against HPV is a promising therapeutic option with fewer side effects. A peptide derived from the HPV-16 E7 protein, called 8Qm, in combination with adjuvants showed promise as a therapeutic vaccine. Here, the ability of polymerized natural amino acids to act as a self-adjuvating delivery system as a therapeutic vaccine was investigated for the first time. Thus, 8Qm was conjugated to polyleucine by standard solid-phase peptide synthesis and self-assembled into nanoparticles or incorporated in liposomes. The liposome bearing the 8Qm conjugate significantly increased mice survival and decreased tumor growth after a single immunization. Further, these liposomes eradicated seven-day-old well-established tumors in mice. Dendritic cell (DC)-targeting moieties were introduced to further enhance vaccine efficacy, and the newly designed liposomal vaccine was tested in mice bearing 11-day-old tumors. Interestingly, these DCs-targeting moieties did not significantly improve vaccine efficacy, whereas the simple liposomal formulation of 8Qm-polyleucine conjugate was still effective in tumor eradication. In summary, a peptide-based anticancer vaccine was developed that stimulated strong cellular immune responses without the help of a classical adjuvant.

Keywords: cervical cancer; antitumor peptide vaccine; poly(amino acid); liposome; mannose-based targeting moiety



Citation: Firdaus, F.Z.; Bartlett, S.; Hussein, W.M.; Lu, L.; Wright, Q.; Huang, W.; Nahar, U.J.; Yang, J.; Khongkow, M.; Veitch, M.; et al. Liposomal Formulations of a Polyleucine–Antigen Conjugate as Therapeutic Vaccines against Cervical Cancer. *Pharmaceutics* **2023**, *15*, 602. <https://doi.org/10.3390/pharmaceutics15020602>

Academic Editors: Noriyasu Kamei and Benjamí Oller-Salvia

Received: 12 January 2023

Revised: 6 February 2023

Accepted: 8 February 2023

Published: 10 February 2023



Copyright: © 2023 by the authors. Licensee MDPI, Basel, Switzerland. This article is an open access article distributed under the terms and conditions of the Creative Commons Attribution (CC BY) license (<https://creativecommons.org/licenses/by/4.0/>).

1. Introduction

Over 600 thousand people are diagnosed with cervical cancer each year triggered by the human papilloma virus (HPV), and 342 thousand people died worldwide as a result of the disease in 2020 alone [1]. Over the past few decades, the number of HPV-related cancer cases has risen, especially in developing countries. While early identification through comprehensive cervical screening programs has decreased the prevalence of cervical cancer, these resources are less accessible in under-developed countries. Treatment options currently available for cervical cancer include chemotherapy, radiotherapy and surgery. However, these treatments have a high failure rate due to significant relapse rates and the development of drug resistance. A prophylactic vaccine has been developed against HPV infection, which will likely decrease the overall rate of cervical cancer; however,

population-scale effects from this vaccine are thought to be at least 20 years away [2]. Furthermore, the risk of people already infected with HPV developing cervical cancer is high. Therefore, the development of a therapeutic vaccine that targets HPV-infected cells is important for treating established cervical cancer and other HPV-associated cancers.

Vaccines designed to treat cancer need to stimulate cytotoxic T-lymphocyte (CTL) responses in order to eliminate abnormal cells bearing specific tumor antigens. The use of whole-HPV or the HPV oncoprotein as an antigen can lead to oncogenic changes. Therefore, the development of a peptide-based vaccine has been suggested [3–5]. The HPV E7 oncoprotein is found in HPV-infected cells and is responsible for HPV-associated tumor cell growth; furthermore, it is the most commonly targeted antigen for therapeutic vaccine development [6–9]. **8Qm** (E744–57, QAEPDRAHYNIVTF), a peptide epitope derived from HPV-16E7 oncoprotein, which is recognized by CD4+ and CD8+ T-lymphocytes, has been shown to have a therapeutic effect against cervical cancer in mice [10,11]. Peptides alone, including **8Qm**, are not able to stimulate any significant immune response due to their poor immunogenicity and low stability in vivo. Instead, peptides need to be incorporated into a delivery system or co-administered with adjuvants to produce an effective vaccine. However, problems associated with the use of currently available adjuvants are common, including toxicity, low efficacy and a limited choice of adjuvants appropriate for human use [12,13]. Moreover, most of the clinically investigated subunit vaccines are unable to elicit strong CD8+ T-cell responses [14], and FDA-approved adjuvants are usually poor CD8+ T-cell activators [15]. Therefore, developing novel adjuvants (or delivery systems) with potent immunomodulatory effects on the cells of the innate and adaptive immune systems without adverse toxicity at therapeutic doses is of great importance in the field of cancer immunotherapy. To date, vaccines assessed in clinical trials have struggled to eliminate advanced cancers and, consequently, no clinically approved therapeutic cancer vaccines currently exist (excluding the vaccine-like dendritic-cell-based treatment sipuleucel-T [Provenge®] for prostate cancer) [16].

Previously, we demonstrated that **8Qm** conjugated to polyacrylates self-assembled to form microparticles. These microparticles, following a single immunization, triggered the eradication of young (three-day-old) tumors in mice [10,11,17]. However, when vaccination was delayed to seven days after tumor implantation, mouse survival rate dropped significantly, even when booster immunizations were administered [18]. Excitingly, after the **8Qm**-polyacrylate conjugate was formulated into liposomes (**L1**), the tumor eradication potency was improved, with three out of five mice being tumor-free 2 months after tumor implantation [19]. However, polyacrylates are not biodegradable, have undefined stereochemistry and contain a variable number of repeating monomer units in each polymer. Considering the shortcomings of synthetic polymers, we designed fully defined and biodegradable polymers built from natural hydrophobic amino acids (pHAAs) that can be synthesized using classic solid-phase peptide synthesis (SPPS) [20]. This method is fully automated and used to incorporate desired peptide epitopes into molecules within a single procedure. Moreover, pHAAs, such as poly-leucine (**pLeu**), mimic the transmembrane fragments of proteins, which are often leucine-rich and, therefore, have been used as anchoring moieties for the incorporation of peptide antigen in liposomal delivery systems [21]. While pHAA systems are still classified as polymeric, they are tremendously different to other polymeric systems currently used for vaccine delivery [22]. The application of fully defined natural hydrophobic amino acids serving as monomers may overcome all disadvantages of classic polymer-based delivery systems. We have demonstrated that a pHAA sequence consisting of **pLeu** conjugated to the J8 B-cell epitope from group A *Streptococcus* self-assembled into nanoparticles stimulated the production of high titers of opsonic antibodies in mice [23,24]. Moreover, **pLeu**-based peptide vaccines were very effective in triggering humoral immunity against hookworm and in parasite clearance from infected animals [25–27]. Here, we hypothesize that **pLeu** can be also employed in a conjugation-based delivery system to induce cytotoxic T-lymphocyte (CTL) responses. Moreover, **pLeu**

conjugates anchored to DC-targeting liposomes were expected to demonstrate improved anticancer efficacy.

The aim of this study was to develop a new antitumor vaccine based on a novel polymeric/liposomal delivery system and demonstrate its efficacy against cervical cancer. **pLeu** was attached to the **8Qm** peptide to form **pLeu-8Qm**, and it was then anchored into a secondary delivery system involving liposomes. A variety of dendritic cell (DC)-targeting moieties were further incorporated into these liposomes to potentially enhance the vaccine's efficacy (Figure 1).

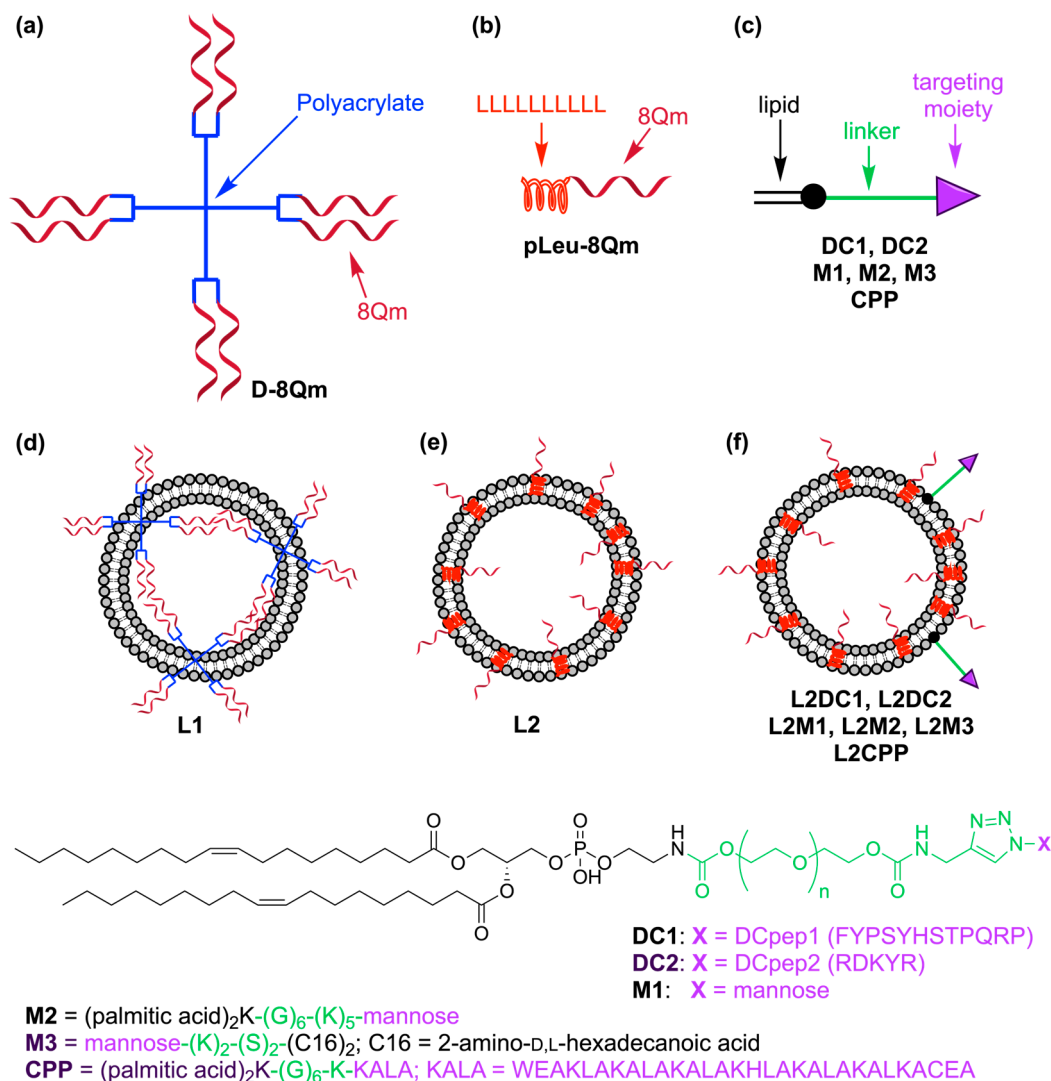


Figure 1. Schematic representation of the vaccine candidates used in the study: (a) **D-8Qm**; (b) **pLeu-8Qm**; (c) DCs-targeting moieties and liposomes; (d) **L1** bearing **D-8Qm**; (e) **L2** bearing **pLeu-8Qm**; and (f) **L2M** bearing **pLeu-8Qm** and targeting moieties. Peptide sequences are shown with their one-letter amino acid code.

2. Materials and Methods

2.1. Materials

All chemical materials used in this study were analytical grade unless otherwise stated. Protected Fmoc amino acids and 1-[bis(dimethylamino)methylene]-1H-1,2,3-triazolo [4,5-b] pyridinium 3-oxide hexafluorophosphate (HATU) were purchased from Mimotopes (Melbourne, VIC, Australia). Dichloromethane (DCM), diethyl ether, piperidine, trifluoroacetic acid (TFA), N,N'-dimethylformamide (DMF), N,N'-diisopropylethylamine (DIPEA), HPLC

grade acetonitrile and methanol were purchased from Merck (Darmstadt, Germany). Triisopropylsilane (TIS), acetic anhydride, erythrocyte lysing buffer, pilocarpine, phosphate-buffered saline (PBS), phenylmethyl-sulfonylfluoride (PMSF), anti-mouse IgG and IgA conjugated to horseradish peroxidase were purchased from Sigma-Aldrich (St. Louis, MO, USA). IC fixation buffer and phenol-free IMDM Glutamax medium were obtained from Gibco®Life Technologies (Carlsbad, CA, USA). Dipalmitoylphosphatidylcholine (DPPC), cholesterol, dimethyldioctadecylammonium bromide (DDAB), Avanti mini extruder, PC membranes and filter supports were bought from Avantis Polar, Inc. (Auspep Pty Ltd., Tullamarine, VIC, Australia). Copper wires were purchased from Aldrich (Steinheim, Germany). All other reagents were obtained at the highest available purity from Sigma-Aldrich (Castle Hill, NSW, Australia).

ESI-MS was performed using a Perkin Elmer Sciex API 3000 instrument with Analyst 1.4 software (Applied Biosystems/MDS Sciex, Toronto, ON, Canada). Analytical RP-HPLC was performed using Shimadzu (Kyoto, Japan) instrumentation (DGU-20A5, LC-20AB, SIL-20ACHT, SPD-M10AVP) with a 1 mL/min flow rate and detection at 214 nm and/or an evaporative light-scattering detector (ELSD). Separation was achieved using a 0–100% linear gradient of solvent B over 40 min on either a Vydac analytical C4 column (214TP54; 5 μ m, 4.6 mm \times 250 mm) or a Vydac analytical C18 column (218TP54; 5 μ m, 4.6 mm \times 250 mm), where solvent A was 0.1% TFA/H₂O and solvent B was 90% MeCN/0.1% TFA/H₂O. Preparative RP-HPLC was performed on Shimadzu (Kyoto, Japan) instrumentation (either LC-20AT, SIL-10A, CBM-20A, SPD-20AV, FRC-10A or LC-20AP \times 2, CBM-20A, SPD-20A, FRC-10A) in linear gradient mode using a 5–20 mL/min flow rate with detection at 230 nm. Separations were performed with solvent A and solvent B on a Vydac preparative C18 column (218TP1022; 10 μ m, 22 mm \times 250 mm), Vydac semi-preparative C18 column (218TP510; 5 μ m, 10 mm \times 250 mm) or Vydac semi-preparative C4 column (214TP510; 5 μ m, 10 mm \times 250 mm). The particle size distribution and measurement of the average particle size were analyzed by dynamic light scattering (DLS) (Malvern Instruments, Malvern, UK). Multiplicate measurements were taken, and the average particle size calculated. MALDI-TOF mass spectrometry samples (1 mg/mL) were spotted onto a MALDI plate with α -cyano-4-hydroxycinnamic acid matrix. A blend of peptide and protein calibrants (Bruker, Billerica, MA, USA) was used for external calibration. MALDI-TOF MS was acquired on a Bruker Autoflex III in negative modes (linear) across a mass range of 2000–10,000 m/z , with spectra gated to 2000 m/z .

2.2. Synthesis of Peptides, Conjugates and Targeting Moieties

D-8Qm and **8Qm** were synthesized as reported previously [19].

Synthesis of pLeu-8Qm

pLeu-8Qm was synthesized by manual stepwise SPPS on rink amide MBHA resin (substitution ratio: 0.52 mmol/g, 0.1 mmol scale, 0.192 g) using HATU/DIPEA Fmoc-chemistry according to the standard procedure [28]. The product was purified using an RP-HPLC C4 column with a 50–80% solvent B gradient over 30 min. t_R = 32.0 min, purity >95%. Yield: 32%. ESI-MS: m/z 1417.7 (calculated 1417.2) $[M+2H]^{2+}$; 945.7 (calculated 945.2) $[M+3H]^{3+}$; MW = 2832.48 (Supporting Information, Figure S1).

Synthesis of DC1

DOPE-PEG3.4k-alkyne (Supporting Information, Figure S2) was synthesized in the same manner as we previously reported [29]. Azido-acetic-acid-modified peptides DCpep1 (N3CH2C(O)-FYPSYHSTPQRP) and DCpep2 (N3CH2C(O)-RDKYR) were synthesized using a standard protocol [28]. The peptides were individually conjugated to compound **4** using copper (I)-catalyzed alkyne azide 1,3-dipolar cycloaddition (CuAAC) following our standard method [30]. Namely, azido-acetic-acid-modified DCpep1 (3.7 mg, 2.4 μ mol, 2.4 equiv.) and DOPE-PEG3.4k-alkyne (4.2 mg, 1.0 μ mol, 1.0 equiv.) were dissolved in DMF (1 mL) and added to the pre-washed and dried copper wires (60 mg). The reaction mixture was degassed with nitrogen and stirred for three hours at 50 °C in the dark under an atmosphere of nitrogen. The copper wire was removed by filtration and washed using

DMF (0.5 mL) before the reaction solution was slowly added (0.005 mL/min) to water (3 mL) to form micelles by the self-assembly process. The formed particles were extensively dialyzed against water in a 2 kDa dialysis bag for three days. Following lyophilization, compound **DC1** was formed as a white powder and characterized using MALDI-TOF mass spectrometry. Compound **DC1** yield: 71%. Purity: 99%. Molecular Weight: 5778. MALDI-TOF: $MW_{\text{calculated average}} = 5779$; $MW_{\text{found}} = 5780$ (Supporting Information, Figure S3).

Synthesis of DC2

Azido-acetic-acid-modified DCpep2 (3.3 mg, 3.6 μmol , 4 equiv.) and DOPE-PEG3.4k-alkyne (3.8 mg, 0.9 μmol , 1.0 equiv.) were dissolved in DMF (1 mL). The rest of the **DC2** synthesis was carried out in an identical manner to that described for the synthesis of **DC1**. Yield: 63%. Compound **DC2** yield: 63%. Purity: 99%. Molecular Weight: 5134. MALDI-TOF: $MW_{\text{calculated average}} = 5135$; $MW_{\text{found}} = 5136$ (Supporting Information, Figure S3).

Synthesis of M1

DOPE-PEG3.4k-alkyne was conjugated to mannose azide [31] using CuAAC reaction following our standard method [30]. The production of **M1** was confirmed with MALDI-TOF analysis. Compound **M1** yield: 37%. Purity: 99%. Molecular Weight: 4509. MALDI-TOF: $MW_{\text{calculated average}} = 4510$; $MW_{\text{found}} = 4502$ (Supporting Information, Figure S4).

Synthesis of M2, M3 and CPP

Synthesis of these lipopeptides was performed as reported [31,32].

2.3. Formulation of Vaccine Candidates

Formulation of L1

D-8Qm and liposomes **L1** were formulated as previously reported [19].

Formulation of pLeu-8Qm

pLeu-8Qm was dissolved in Millipore endotoxin-free water (900 μL) and self-assembled into nanoparticles. Prior to injection, PBS (100 μL , 10 \times) was added to the formulation, producing the final concentration of 1 mg/mL.

Formulation of L2

Dipalmitoylphosphatidylcholine (DPPC), didodecyltrimethylammonium bromide (DDAB) and cholesterol were each dissolved in chloroform (1 mL) to achieve final concentrations of 10 mg/mL, 10 mg/mL and 5 mg/mL, respectively. Solutions of DPPC (0.5 mL), DDAB (0.2 mL) and cholesterol (0.2 mL) were added to a round-bottom flask containing chloroform (2 mL). **pLeu-8Q** (1 mg) was dissolved in methanol (1 mL) and added to the flask. The solvents were then slowly evaporated under reduced pressure using a rotatory evaporator before the residual solvent was removed under vacuum overnight generating a lipid film. The lipid film was rehydrated with Millipore endotoxin-free water (900 μL) at 56 $^{\circ}\text{C}$ following extrusion with 200 nm pore-size polycarbonate membrane. Prior to injection, PBS (100 μL , 10 \times) was added to the formulation, producing the final concentration of **pLeu-8Qm** (1 mg/mL) in **L2**. The encapsulation efficiency of **pLeu-8Qm** in liposomes was 99%. Encapsulation was determined as previously reported [19].

Formulation of L2M1, L2M2, L2M3, L2DC1 and L2DC2

Liposomes bearing targeting moieties were formulated in a similar manner to **L2**, except DC-targeting moieties **M1** (0.233 mg), **M2** (0.063 mg), **M3** (0.098 mg), **DC1** (0.299 mg), **DC2** (0.265 mg) and **CPP** (0.259 mg) in equimolar quantities, which were added along with **pLeu-8Q** to the lipid solution. Lipid film was rehydrated with Millipore endotoxin-free water (900 μL) at 56 $^{\circ}\text{C}$ following extrusion with a 200 nm pore-size polycarbonate membrane. Finally, PBS (100 μL , 10 \times) was added to the formulation, producing **pLeu-8Qm** (1 mg/mL) in unilamellar liposomal formulations.

Formulation of L2CPP

The liposomes bearing targeting moieties were formulated in a similar manner to **L2**, except DC-targeting moieties **CPP** (0.25 mg)—added along with **pLeu-8Q** to the lipid solution. In addition, DDAB was excluded from lipid solution. Lipid film was rehydrated with 900 μL of Millipore endotoxin-free water at 56 $^{\circ}\text{C}$ and not extruded. Finally, 100 μL of

10× PBS was added to the formulation, producing the final concentration of **pLeu-8Qm** (1 mg/mL) as multilamellar liposomes.

2.4. Characterization of Nanoliposomes

Particle size, zeta potential and polydispersity of the vaccine candidates were measured by dynamic light scattering (DLS) using a Zetasizer (Nano ZX, Malvern, UK). Measurements were taken at 25 °C and 173° light scattering. DLS measurements were taken using a Zetasizer Nano ZP instrument (Malvern Instrument, UK) with Malvern Zetasizer Analyzer 6.2 software. Particle morphology was examined using transmission electron microscopy (TEM) (HT7700 Exalens, HITACHI Ltd., Tokyo, Japan) after vacuum drying. Briefly, samples were diluted in pure distilled water (1:100), dropped directly onto glow-discharged carbon-coated copper grids, then stained with uranyl acetate (2%). Samples were observed at 200.0 k× magnification.

2.5. Mice and TC-1 Cell Lines

TC-1 cells (murine C57BL/6 lung epithelial cells transformed with HPV-16 E6/E7 and ras oncogenes) were obtained from TC Wu, John Hopkins Cervical Cancer Research Lab, USA. TC-1 cells were cultured and maintained at 37 °C/5% CO₂ in RPMI 1640 medium supplemented with 10% heat-inactivated fetal bovine serum. Female C57BL/6 (6–8-week-old) mice were purchased from the Animal Resources Centre (Perth, Western Australia). Animal experiments were approved by The University of Queensland Animal Ethics Committee (UQDI/TRI/351/15 and UQDI/032/20) and were carried out in accordance with National Health and Medical Research Council (NHMRC) of Australia guidelines.

2.6. In Vivo Tumor Treatment Experiments

C57BL/6 Female mice (8 mice per group in pilot study, and 6 mice per group in the second study) were challenged subcutaneously in the flank with 2×10^5 TC-1 tumor cells/mouse (i.e., 1×10^5 TC-1 tumor cells/site). After 7 days (pilot) or 11 days (second study), mice were injected in the flank with the vaccine candidates. Each mouse received peptide (100 µL) or liposome formulation containing antigen (100 µg). Mice also received PBS (100 µL, 1×) as a negative control. **L1** or a formulation containing **8Qm** (100 µg) and CpG ODN 1826 adjuvant (20 µg) dissolved in PBS were used as a positive control. Each mouse received a single dose of the vaccine/control solution. Tumor size was measured (by palpation and calipers) and recorded for each mouse every 2 days. Tumor volume was calculated using the formula: $V \text{ (cm}^3\text{)} = 3.14 \times [\text{largest diameter} \times (\text{perpendicular diameter})^2]/6$. The average tumor size per group (n = 8 or 6) was also calculated. Mice were euthanized when tumors reached 1 to 3 cm or if they started bleeding to avoid unnecessary suffering. An additional cohort of C57BL/6 mice (6 mice per group) were immunized with antigens, as described above. Mouse spleens were collected from these animals 10 days post immunization and used for the ELISPOT assay.

2.7. IFN-Gamma ELISPOT Assays

ELISPOT plates were coated with 5 µg/mL IFN-γ capture antibody (clone 14-7313-85 eBioscience, San Diego, CA, USA) in PBS at 4 °C overnight. The plates were then blocked with RPM/20% fetal bovine serum at room temperature for 3 h. Splenocytes from C57BL/6 mice were harvested from the spleens of naïve and immunized mice. The red blood cells were depleted using red blood cell lysing buffer (0.155 M ammonium chloride in 0.01 M Tris-HCl buffer, Sigma). Splenocytes were then resuspended in RPMI (Sigma) supplemented with 20% FACs (100 U/mL penicillin, 100 µg/mL streptomycin and 50 µM β-mercaptoethanol). The cells were plated at 5×10^5 cells per well in triplicate on ELISPOT plates. The E7 peptide (10 µg/mL) was added alongside 10 ng/mL rhIL-2 to a final volume of 200 µL per well. Plates were incubated for 8 h at 37 °C and washed. Biotinylated IFN-γ detection antibody (2 µg/mL; clone R4-6A2; eBioscience) in BSA (1%) was then added

at room temperature. The plates were washed, and bound cytokine was visualized with 3-amino-9-ethylcarbazole. Spots were counted with an ELISPOT reader.

2.8. Statistical Analysis

All data were analyzed using GraphPad Prism 7 software. Kaplan–Meier survival curves were used to compare tumor treatment candidates. Differences in survival treatments were determined using the log-rank (Mantel–Cox) test, with $p < 0.05$ considered statistically significant. ELISPOT statistical analysis was performed using a one-way analysis of variance (ANOVA) followed by Tukey’s multiple comparisons test (ns, $p > 0.05$; *, $p < 0.05$).

3. Results and Discussion

3.1. Vaccine Design

In our previous attempts to develop efficient vaccine delivery systems, we have demonstrated that conjugation of the polyleucine moiety to a peptide antigen greatly enhanced antigen-specific humoral immune responses [20,21,23–27]. We also found that the polymer–antigen conjugate **D-8Qm** once formulated into liposomes (**L1**) was able to eradicate, to some extent, seven-days-old cancer in mice [27]. Herein, we have replaced the polyacrylate dendrimer (**D**) with polyleucine to produce the self-assembling conjugate, **pLeu-8Qm**. In addition, we have also combined the polyleucine strategy with a liposomal formulation applied for **D-8Qm** (**L1**) to produce **L2**. To further improve vaccine efficacy, we anchored a variety of DC-targeting moieties to **L2** liposomes (Figure 1), as antigen uptake by DCs (and other antigen presenting cells) is a key process in initializing natural immune responses, including anticancer cellular immunity [33]. All the targeting moieties have been lipidated to allow their anchoring to liposomes. Here, lipopeptides **D1** and **D2** were bearing DCpep-1 and DCpep-2 epitopes, respectively, where both DCpep-1 and DCpep-2 are reported to have DC-targeting properties [34]. In addition, DCpep-1 has been shown to stimulate specific T-cell responses against tumors [35–37], while DCpep-2 regulated inflammatory mediators [38,39]. The incorporation of a mannose-based ligand into liposome formulations has been previously reported as being effective in promoting CTL responses [40–42]. We designed our ligands (**M1–M3**) to have different spacer lengths between the mannose and lipidic moieties, where the importance of these spacers has been previously reported [3,43–45]. We have also demonstrated the mechanism of mannose-receptor-mediated uptake [46]. Importantly, the ability of **M2** anchored into liposomes to greatly enhance humoral immune responses against a bacterial antigen has also been proven (unpublished data). Along the same line, we also demonstrated that the mannose–lipid conjugate **M3** easily anchored into liposomes induced cellular immunity against malaria and babesia parasites [31,47–49]. Finally, we had also previously proven that the lipidated-cell-penetrating peptide **KALA** (**CPP**), upon anchoring to liposomes, triggered the production of opsonic antibodies against a co-anchored peptide antigen [32]. The ability of cell-penetrating peptides to improve the cellular immunity of the co-delivered antigen has also been reported by other groups [50]. Identically produced cationic liposomes were used in all formulations (**L1**, **L2**, **L2DC1**, **L2DC2**, **L2M1**, **L2M2**, **L2M3**) except **L2CPP**, where neutral multilamellar liposomes were applied. Here, the use of cationic liposomes in combination with a **CPP** was redundant due to the very high cationic charge of the **KALA** peptide, and a **CPP** was more effective when combined with multilamellar (not unilamellar) liposomes [32].

3.2. Vaccine Preparation

All the peptide components of vaccines and targeting moieties were synthesized using Fmoc-SPPS. **pLeu-8Qm** was also produced as a single molecule using the standard SPPS methodology. **pLeu-8Qm** was incorporated in DC-targeting liposomal formulations and used for a pilot immunization study. The polymeric conjugate **D-8Qm** was produced by conjugation of the **8Qm** peptide to polyacrylate **D** by the copper-catalyzed alkyne–azide

cycloaddition (CuAAC) reaction and self-assembled into particles by the solvent replacement method, as previously reported [19,51]. Dialysis was performed in water for three days to remove residual peptide, copper and organic solvents, and elemental analysis was used to confirm the formation of the product, which was in line with the methods of many previous studies [10,11,20,51,52], as the conjugate contained a higher nitrogen/carbon ratio compared with the polyacrylate alone. Theoretical and observed (nitrogen [N]/carbon [C]) ratios were used to calculate the exact substitution of the polymer core with the peptide epitopes. The observed nitrogen–carbon ratio for **D-8Qm** (N/C = 0.115) was higher than that of the polymer alone (N/C = 0.017) and corresponded to 83% of the substitution rate of the dendrimer with **8Qm** peptide (similar to that previously reported at 85% [19]). Both **D-8Qm** and **pLeu-8Qm**, as amphiphilic conjugates, were easily incorporated (anchored) into liposomes [19,21] to form **L1** and **L2**, respectively (Figure 1).

DCs-targeting moieties, **DC1**, **DC2** and **M1**, were designed to anchor targeting moieties, DCpep1, DCpep2 and mannose, to liposomes by the DOPE lipid and PEG linker for optimal receptor recognition (Figure 1) [53]. First, DOPE-PEG3.4k-alkyne was synthesized using our published procedure (Supporting Information, Figure S2) [29] before being individually reacted with azide derivatives of DCpep1, DCpep2 and mannose to produce **DC1**, **DC2** and **M1**, respectively (Supporting Information, Figures S3 and S4). Other targeting moieties (**M2**, **M3** and **CPP**) were synthesized as reported [31,32]. The conjugates **D-8Qm** and **pLeu-8Qm**, as well as the lipidated targeting moieties (**DC1**, **DC2**, **M1**, **M2**, **M3**, **CPP**), were incorporated into the liposomal bilayer during a thin-film lipid formulation. Lipid films were hydrated and sonicated to produce **L1**, as previously reported [19], or extruded (**L2**, **L2DC1**, **L2DC2**, **L2M1**, **L2M2**, **L2M3**) with 200 nm pore membranes to form uniform-sized liposomes, except **L2CPP**, which was formulated as multilamellar liposomes (extrusion step was omitted during liposomes preparation).

The size and surface charge of the vaccine candidates were analyzed using DLS (Table 1, Supporting Information, Figure S5). Both **D-8Qm** and **pLeu-8Qm** produced aggregates of sub/micron sizes with high polydispersity (polydispersity index; PDI = 0.6–0.7) and a similar negative charge ($\zeta = -10$ – -14 mV). In contrast, all liposome formulations were positively charged and relatively monodispersed, except **L1** and **L2CPP**. Unilamellar liposomes bearing **pLeu-8Qm** were produced in the size range of 150–200 nm, which was typically more immunogenic compared with larger-sized particles [54–56]. Multilamellar liposome **L2CPP** formed submicron particles (0.6 μm , PDI = 0.4) with a high positive charge. Additionally, the size and morphology of the vaccine candidates were analyzed by TEM (Supporting Information, Figure S6). Large particle aggregates were detected on images of **D-8Qm**, while all liposomes formed typical spherical liposome structures, which were uniform in size (100–250 nm) without visible traces of large aggregates, as detected by DLS in the case of **L1** and **L2DC1** (Supporting Information, Figure S5).

Table 1. Physicochemical characterization of vaccine candidates.

Vaccine	Targeting Moiety	Size (nm \pm SD)	PDI	Charge (mV \pm SD)
Blank liposomes	-	165 \pm 4	0.06 \pm 0.01	61 \pm 2
D-8Qm	-	250 \pm 50; 1500 \pm 100	0.70 \pm 0.06	-14 \pm 1
pLeu-8Qm	-	750 \pm 350	0.60 \pm 0.10	-10 \pm 5
L1	-	320 \pm 20; 4500 \pm 600	0.50 \pm 0.05	28 \pm 2
L2	-	157 \pm 2	0.10 \pm 0.01	24 \pm 2
L2DC1	DC1	200 \pm 10; 3200 \pm 1100	0.30 \pm 0.01	17 \pm 2
L2DC2	DC2	160 \pm 10	0.05 \pm 0.01	23 \pm 2
L2M1	M1	162 \pm 6	0.10 \pm 0.01	13 \pm 1
L2M2	M2	174 \pm 2; 4800 \pm 300	0.20 \pm 0.01	20 \pm 1
L2M3	M3	143 \pm 2	0.05 \pm 0.01	23 \pm 2
L2CPP ¹	CPP	610 \pm 60	0.40 \pm 0.03	54 \pm 5

¹ Liposome formulation **L2CPP** did not include the cationic lipid (DDAB) and was not extruded.

3.3. Immunological Evaluation of the Vaccine Candidates

At first, the therapeutic effect of the vaccine candidates on established tumors was evaluated in eight-week-old female C57BL/6 mice seven days post TC-1 tumor implantation (Figure 2). Average tumor growth was fast, with only 25% of the negative control (PBS-treated) mice surviving to day 21. Alone, **pLeu-8Qm** decreased tumor growth and prolonged mouse survival. The incorporation of **pLeu-8Qm** into liposomes (**L2**) greatly improved vaccine efficacy. While all mice treated with **L2** survived 64 days, two of the eight mice had tumor growth recurrence after days 34 and 56. The improved ability of the liposome-based **L2** vaccine candidate in triggering an antitumor immune response compared with **pLeu-8Qm** alone might be attributed to the size of the particles. **pLeu-8Qm** formed highly polydisperse submicroparticles, while **L2** formed nanoparticles (<200 nm); however, smaller particles are widely reported to be more immunogenic [57,58].

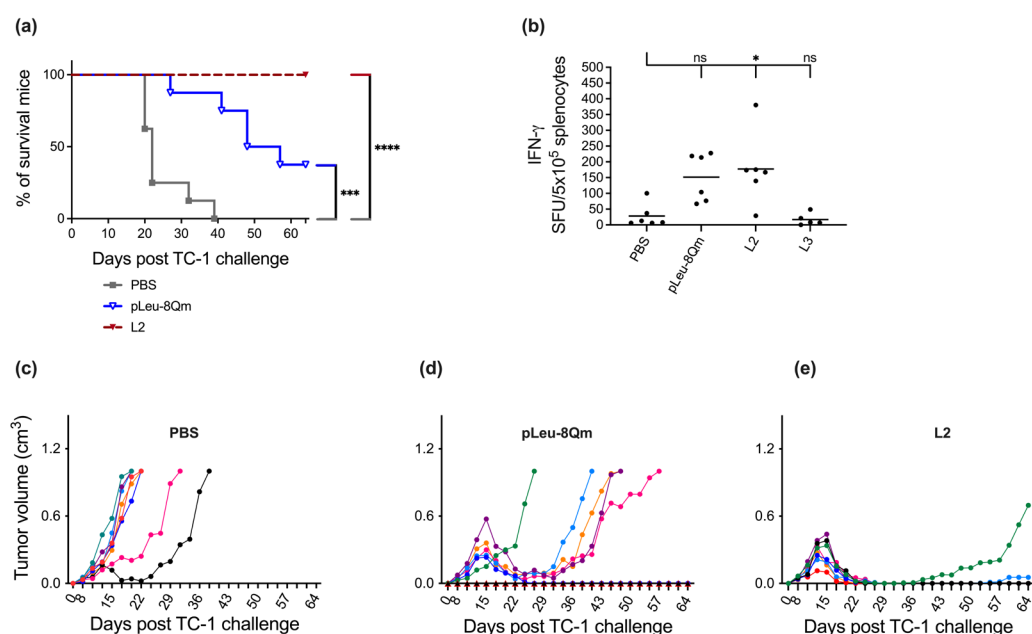


Figure 2. In vivo tumor treatment experiments and CD8⁺ T-cell activation. C57BL/6 mice ($n = 8$ mice/group) were inoculated subcutaneously with TC-1 tumor cells (day 0) and vaccinated with different immunogens on day 7. (a) Survival rate was monitored and time to death plotted on a Kaplan–Meier survival curve. Tumor volume was monitored and plotted for each individual mouse immunized with (b) PBS; (c) **pLeu-8Qm**; (d) **L2**. The survival rate of each group was compared with the negative control (PBS) and was analyzed using the log-rank (Mantel–Cox) test (** $p < 0.001$; **** $p < 0.0001$). (e) Assessment of CD8⁺ T-cell responses in mice subcutaneously immunized with the vaccine candidates. Mouse spleens were harvested ten days after vaccination and IFN- γ production in response to short E749-57 (RAHYNIVTF) CD8 peptide epitope was determined by ELISPOT ($n = 6$ mice/group). The **L3** group (irrelevant control) was identical to **L2** except the antigen **8Qm** was replaced with J8 B-cell epitope derived from group A streptococcus (unrelated epitope). ELIPOST data were pooled from two independent experiments and analyzed using one-way ANOVA followed by Tukey’s post hoc multiple comparison test (ns, $p > 0.05$; *, $p < 0.05$).

As the vaccine candidates investigated in this study aimed to stimulate CD8⁺ CTLs in order to eradicate HPV-infected cells, the recall of IFN- γ production by CD8⁺ T-cells was examined in immunized mice in response to MHC class I-restricted E7 peptide re-stimulation by ELISPOT (Figure 2). The immunization of mice with **pLeu-8Qm** delivered by liposomes induced significantly higher levels of IFN- γ compared with PBS, corresponding with its antitumor potency. This demonstrated that the downstream priming of the T-cells via IFN- γ activation led to the eradication of tumors following subcutaneous immunization. Moreover, this antitumor efficacy was achieved without the presence of an external adju-

vant, assistance of chemotherapy, multiple immunizations and/or boosting with immune checkpoint inhibitors [59–62].

Encouraged by the outcomes of the pilot study, we designed several new vaccine candidates (Figure 1) and examined them under more demanding conditions (Figure 3, Supporting Information, Figure S7). The efficacy of the vaccine candidates was evaluated by testing against 11-day-old tumors following a single immunization to demonstrate the superiority of the strategy compared with our previous studies. These previous studies utilized 8Qm-based peptide–polymer conjugate vaccines targeting 3-day-old smaller tumors [11], a prime-boost immunization schedule using HPV E6- and E7-epitope-based multivalent conjugates with a booster [18], or the use of 8Qm emulsified in the commercialized adjuvant, Montanide ISA 51, to achieve significant antitumor effects [10]. Previously examined polyacrylate-based vaccine **D-8Qm** and its liposomal formulation **L1** have also been assessed. In addition, the classical “cellular” adjuvant, CpG, was used as a positive control. CpG has been recently extensively investigated as an effective immune stimulator in the development of therapeutic vaccines against HPV-related cancers [4,7,63–65]. Three vaccine candidates, **L2**, **L2DC1** and **L2M2**, delayed tumor regrowth and induced tumor regression with the highest survival rate (67% on day 60). All surviving mice treated with **L2** achieved complete tumor regression on day 60, while full tumor regression was observed in three out of six mice in both **L2DC1** and **L2M2** (Figure 3). Moreover, **L2M2** induced some tumor regression in all mice, and these mice survived up to day 47 following a single immunization. Importantly, all three vaccines (**L2**, **L2DC1** and **L2M2**) were significantly more effective as therapeutic vaccines than **8Qm** adjuvanted with CpG. Mice immunized with **8Qm**/CpG showed a delay in tumor growth compared with the negative control (PBS); however, they ultimately had the same survival rate of 0% on day 60. Among the three leading formulations, even the simple liposome formulation **L2** was more effective at inducing tumor regression than the previous leading vaccine candidates, **D-8Qm** and **L1** [19]. It is also worth noting that when unconjugated and adjuvant-free 8Qm was incorporated into the same liposomal formulation, therapeutic potential was not observed [19]. Other DC-targeting formulations (**L2DC2**, **L2M1**, **L2M3** and **L2CPP**) were less effective than the untargeted **L2** formulation and not significantly more effective than **8Qm**/CpG. In addition, there was no correlation between the size of liposome particles and vaccine efficacy. The leading vaccine candidates, **L2**, **L2DC1** and **L2M2**, had particle sizes in similar ranges to other liposomal formulations, except **L2CPP** (Table 1).

Notably, targeting moieties did not improve the final survival rate; however, the formulation bearing lipidated mannose (**M2**) delayed tumor growth more significantly than other formulations. Thus, further investigations on this formulation are required. For example, the anticancer efficacy of **L2M2** might be greatly enhanced by the administration of a boosting dose around 3–4 weeks following the primary vaccination.

In our study, mice immunized with **L2**, **L2DC1** and **L2M2** demonstrated improved survival 60 days after the inoculation of the same density of TC1 tumor cells (1×10^5), despite the more advanced stage of tumor development at the time of the initiation of vaccine treatment (11 days post tumor cell inoculation versus 7 or 8 days in other studies [66,67]). Furthermore, within the framework of a single immunization schedule, the **L2**, **L2DC1**- and **L2M2**-immunized mice displayed tumor eradication in some cases, outperforming prior studies utilizing multiple immunizations, which failed to achieve complete tumor regression [66–68]. Additionally, the efficacy of our vaccine formulation was maintained without the use of multiepitopes from both E6 and E7 proteins [69]; the addition of adjuvants, such as flagellin [70], Montanide ISA 720 [71] or a combination of poly I:C and CpG [63]; or synergistic therapy with immune checkpoint inhibitors, such as anti-CTLA4 [72] or anti-PD1 [73].

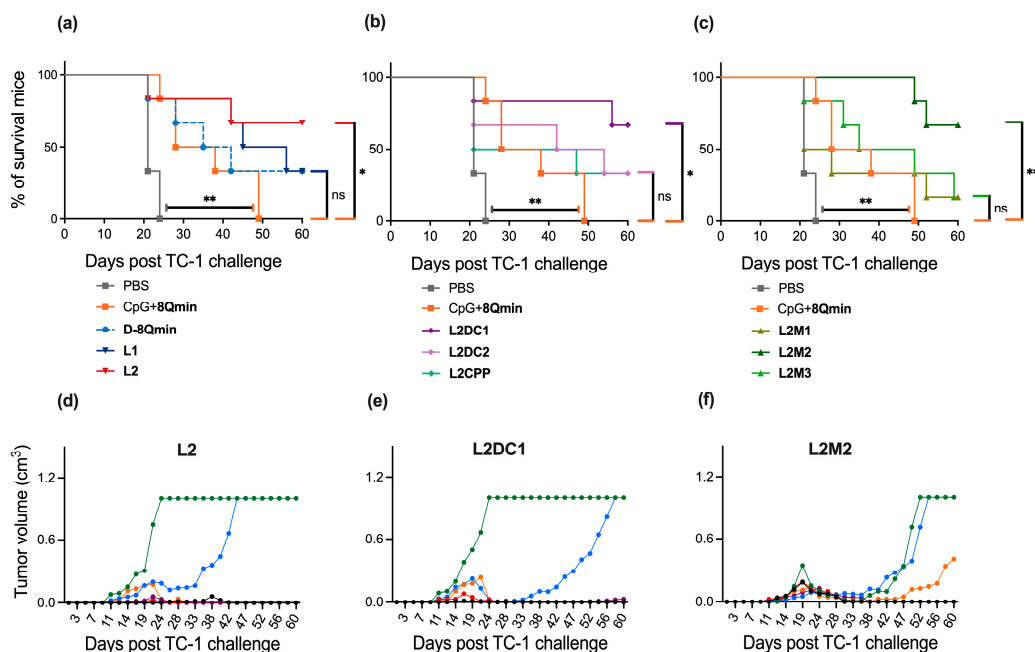


Figure 3. In vivo tumor treatment experiments. C57BL/6 mice ($n = 6$ mice/group) were inoculated subcutaneously with TC-1 tumor cells (day 0) and vaccinated with different immunogens on day 11. (a–c) Survival rate was monitored and time to death plotted on a Kaplan–Meier survival curve (separated here into three panels for clarity). The survival rate of each group was compared with the positive control (CpG + 8Qm) and was analyzed using the log-rank (Mantel–Cox) test (ns, $p > 0.05$; *, $p < 0.05$; ** $p < 0.01$). Tumor volume was monitored and plotted for each individual mouse immunized with (d) L2; (e) L2DC1; (f) L2M2. Tumor volume charts for other groups are presented in Supporting Information, Figure S7.

4. Conclusions

We demonstrated that a fully defined, natural, hydrophobic amino-acid-based polymer conjugated to peptide antigen acts as an efficient vaccine delivery system. Importantly, polyleucine mimics the transmembrane fragments of proteins, allowing the anchoring of the conjugate to liposomes and effectively triggering cellular immunity to destroy tumor cells following a single immunization without the use of an additional adjuvant. In contrast with nanotechnology-based strategies, which usually offer incompletely defined systems, our strategy utilizes a polymer built from natural amino acids that is both a single molecule and a single isomer. Given the need for the vaccine treatment of intracellular infectious diseases and malignancies, we anticipate numerous applications for the vaccine delivery system presented here.

Supplementary Materials: The following supporting information can be downloaded at: <https://www.mdpi.com/article/10.3390/pharmaceutics15020602/s1>, Figure S1: ESI-MS and HPLC trace of pLeu-8Qm. Figure S2: Synthesis of compound DOPE-PEG3.4k-alkyne (4). **Figure S3:** The MALDI-TOF mass spectrometry of DC1 and DC2. Figure S4: The MALDI-TOF mass spectrometry of DOPE-PEG3.4k-alkyne (4) and DOPE-PEG3400-mannose (M1). Figure S5: Particles size of (A) D-8Qm, (B) pLeu-8Qm, (C) L1, (D) L2, (E) L2DC1, (F) L2DC2, (G) L2M1, (H) L2M2, (I) L2M3 and (J) L2CPP were recorded by dynamic light scattering (DLS). Figure S6: Transmission electron microscopy images of (A) D-8Qm, (B) L1, (C) L2, (D) L2DC1, (E) L2DC2, (F) L2M1, (G) L2M2, (H) L2M3 and (I) L2CPP. Figure S7: In vivo tumor treatment experiments. Tumor volume was monitored and plotted for each individual mouse immunized with PBS, CpG + 8Qm, D8Qm, L1, L2DC2, L2M1, L2M3, and L2CPP.

Author Contributions: Conceptualization, I.T. and M.S.; methodology, J.L.G.C., J.W.W., I.T. and M.S.; formal analysis, F.Z.F., S.B. and L.L.; investigation, F.Z.F., S.B., W.M.H., L.L., U.J.N., Q.W., J.Y. and M.K.; resources, M.J.M., I.T. and M.S.; data curation, F.Z.F., S.B., W.M.H., W.H., M.V. and P.K.;

writing—original draft preparation, F.Z.F., S.B. and L.L.; writing—review and editing, R.J.S., I.T. and M.S.; supervision, W.M.H., U.R.R., M.J.M., R.J.S., I.T. and M.S.; funding acquisition, I.T. and M.S. All authors have read and agreed to the published version of the manuscript.

Funding: This work was supported by the Australian Research Council (ARC; Discovery Project DP210101280).

Institutional Review Board Statement: Animal experiments were approved by The University of Queensland Animal Ethics Committee (UQDI/TRI/351/15) in accordance with National Health and Medical Research Council (NHMRC) of Australia guidelines.

Data Availability Statement: Not applicable.

Acknowledgments: SB is supported by a University of Queensland Research Training Program Scholarship (UQ RTP). The authors acknowledge the facilities and the scientific and technical assistance of the Australian Microscopy and Microanalysis Research Facility at the Centre for Microscopy and Microanalysis, The University of Queensland.

Conflicts of Interest: M.S. and I.T. are co-inventors in a patent application entitled “Self-assembling, self-adjuvating system for delivery of vaccines” filed by the University of Queensland (application number: WO/2021/138721, PCT/AU2021/050012). The remaining authors declare no competing interests.

References

1. Sung, H.; Ferlay, J.; Siegel, R.L.; Laversanne, M.; Soerjomataram, I.; Jemal, A.; Bray, F. Global Cancer Statistics 2020: GLOBOCAN Estimates of Incidence and Mortality Worldwide for 36 Cancers in 185 Countries. *CA A Cancer J. Clin.* **2021**, *71*, 209–249. [[CrossRef](#)] [[PubMed](#)]
2. Maine, D.; Hurlburt, S.; Greeson, D. Cervical cancer prevention in the 21st century: Cost is not the only issue. *Am. J. Public Health* **2011**, *101*, 1549–1555. [[CrossRef](#)]
3. Alharbi, N.; Skwarczynski, M.; Toth, I. The influence of component structural arrangement on peptide vaccine immunogenicity. *Biotechnol. Adv.* **2022**, *60*, 108029. [[CrossRef](#)]
4. Zhang, J.; Fan, J.; Skwarczynski, M.; Stephenson, R.J.; Toth, I.; Hussein, W.M. Peptide-Based Nanovaccines in the Treatment of Cervical Cancer: A Review of Recent Advances. *Int. J. Nanomed.* **2022**, *17*, 869–900. [[CrossRef](#)]
5. Reintjens, N.R.M.; Tondini, E.; de Jong, A.R.; Meeuwenoord, N.J.; Chiodo, F.; Peterse, E.; Overkleeft, H.S.; Filippov, D.V.; van der Marel, G.A.; Ossendorp, F.; et al. Self-Adjuvanting Cancer Vaccines from Conjugation-Ready Lipid A Analogues and Synthetic Long Peptides. *J. Med. Chem.* **2020**, *63*, 11691–11706. [[CrossRef](#)]
6. Van der Maaden, K.; Heuts, J.; Camps, M.; Pontier, M.; van Scheltinga, A.T.; Jiskoot, W.; Ossendorp, F.; Bouwstra, J. Hollow microneedle-mediated micro-injections of a liposomal HPV E7(43–63) synthetic long peptide vaccine for efficient induction of cytotoxic and T-helper responses. *J. Control. Release* **2018**, *269*, 347–354. [[CrossRef](#)]
7. Galliverti, G.; Tichet, M.; Domingos-Pereira, S.; Hauert, S.; Nardelli-Haeffliger, D.; Swartz, M.A.; Hanahan, D.; Wullschlegel, S. Nanoparticle Conjugation of Human Papillomavirus 16 E7-long Peptides Enhances Therapeutic Vaccine Efficacy against Solid Tumors in Mice. *Cancer Immunol. Res.* **2018**, *6*, 1301–1313. [[CrossRef](#)] [[PubMed](#)]
8. Mardani, G.; Bolhassani, A.; Agi, E.; Shahbazi, S.; Mehdi Sadat, S. Protein vaccination with HPV16 E7/Pep-1 nanoparticles elicits a protective T-helper cell-mediated immune response. *IUBMB Life* **2016**, *68*, 459–467. [[CrossRef](#)]
9. Hussein, W.M.; Liu, T.-Y.; Maruthayanar, P.; Mukaida, S.; Moyle, P.M.; Wells, J.W.; Toth, I.; Skwarczynski, M. Double conjugation strategy to incorporate lipid adjuvants into multiantigenic vaccines. *Chem. Sci.* **2016**, *7*, 2308–2321. [[CrossRef](#)] [[PubMed](#)]
10. Liu, T.-Y.; Hussein, W.M.; Giddam, A.K.; Jia, Z.; Reiman, J.M.; Zaman, M.; McMillan, N.A.; Good, M.F.; Monteiro, M.J.; Toth, I.; et al. Polyacrylate-Based Delivery System for Self-adjuvanting Anticancer Peptide Vaccine. *J. Med. Chem.* **2015**, *58*, 888–896. [[CrossRef](#)]
11. Liu, T.Y.; Hussein, W.M.; Jia, Z.F.; Ziora, Z.M.; McMillan, N.A.J.; Monteiro, M.J.; Toth, I.; Skwarczynski, M. Self-adjuvanting polymer-peptide conjugates as therapeutic vaccine candidates against cervical cancer. *Biomacromolecules* **2013**, *14*, 2798–2806. [[CrossRef](#)]
12. Nevagi, R.J.; Toth, I.; Skwarczynski, M. Peptide-based Vaccines. In *Peptide Applications in Biomedicine, Biotechnology and Bioengineering*; Koutsopoulos, S., Ed.; Woodhead Publishing: Oxford, UK, 2018; pp. 327–358.
13. Azmi, F.; Ahmad Fuaad, A.A.; Skwarczynski, M.; Toth, I. Recent progress in adjuvant discovery for peptide-based subunit vaccines. *Hum. Vaccines Immunother.* **2014**, *10*, 778–796. [[CrossRef](#)] [[PubMed](#)]
14. Seder, R.; Reed, S.G.; O’Hagan, D.; Malyala, P.; D’Oro, U.; Laera, D.; Abrignani, S.; Cerundolo, V.; Steinman, L.; Bertholet, S. Gaps in knowledge and prospects for research of adjuvanted vaccines. *Vaccine* **2015**, *33* (Suppl. S2), B40–B43. [[CrossRef](#)]
15. Lambrecht, B.N.; Kool, M.; Willart, M.A.; Hammad, H. Mechanism of action of clinically approved adjuvants. *Curr. Opin. Immunol.* **2009**, *21*, 23–29. [[CrossRef](#)]
16. Mougél, A.; Terme, M.; Tanchot, C. Therapeutic Cancer Vaccine and Combinations With Antiangiogenic Therapies and Immune Checkpoint Blockade. *Front. Immunol.* **2019**, *10*, 467. [[CrossRef](#)] [[PubMed](#)]

17. Liu, T.-Y.; Giddam, A.K.; Hussein, W.; Jia, Z.; McMillan, N.; Monteiro, M.; Toth, I.; Skwarczynski, M. Self-Adjuvanting Therapeutic Peptide-Based Vaccine Induce CD8+ Cytotoxic T Lymphocyte Responses in a Murine Human Papillomavirus Tumor Model. *Curr. Drug Deliv.* **2015**, *12*, 3–8. [[CrossRef](#)]
18. Hussein, W.M.; Liu, T.-Y.; Jia, Z.; McMillan, N.A.; Monteiro, M.J.; Toth, I.; Skwarczynski, M. Multiantigenic peptide-polymer conjugates as therapeutic vaccines against cervical cancer. *Bioorgan. Med. Chem.* **2016**, *24*, 4372–4380. [[CrossRef](#)] [[PubMed](#)]
19. Khongkow, M.; Liu, T.Y.; Bartlett, S.; Hussein, W.M.; Nevagi, R.; Jia, Z.F.; Monteiro, M.J.; Wells, J.W.; Ruktanonchai, U.R.; Skwarczynski, M.; et al. Liposomal formulation of polyacrylate-peptide conjugate as a new vaccine candidate against cervical cancer. *Precis. Nanomed.* **2018**, *1*, 183–193. [[CrossRef](#)]
20. Skwarczynski, M.; Zhao, G.; Boer, J.C.; Ozberk, V.; Azuar, A.; Cruz, J.G.; Giddam, A.K.; Khalil, Z.G.; Pandey, M.; Shibu, M.A.; et al. Poly(amino acids) as a potent self-adjuvanting delivery system for peptide-based nanovaccines. *Sci. Adv.* **2020**, *6*, eaax2285. [[CrossRef](#)]
21. Azuar, A.; Madge, H.Y.R.; Boer, J.C.; Gonzalez Cruz, J.L.; Wang, J.; Khalil, Z.G.; Deceneux, C.; Goodchild, G.; Yang, J.; Koirala, P.; et al. Poly(hydrophobic Amino Acids) and Liposomes for Delivery of Vaccine against Group A Streptococcus. *Vaccines* **2022**, *10*, 1212. [[CrossRef](#)]
22. Nevagi, R.J.; Skwarczynski, M.; Toth, I. Polymers for subunit vaccine delivery. *Eur. Polym. J.* **2019**, *114*, 397–410. [[CrossRef](#)]
23. Azuar, A.; Li, Z.; Shibu, M.A.; Zhao, L.; Luo, Y.; Shalash, A.O.; Khalil, Z.G.; Capon, R.J.; Hussein, W.M.; Toth, I.; et al. Poly(hydrophobic amino acid)-Based Self-Adjuvanting Nanoparticles for Group A Streptococcus Vaccine Delivery. *J. Med. Chem.* **2021**, *64*, 2648–2658. [[CrossRef](#)] [[PubMed](#)]
24. Azuar, A.; Shibu, M.A.; Adilbish, N.; Marasini, N.; Hung, H.; Yang, J.; Luo, Y.; Khalil, Z.G.; Capon, R.J.; Hussein, W.M.; et al. Poly(hydrophobic amino acid) Conjugates for the Delivery of Multiepitope Vaccine against Group A Streptococcus. *Bioconj. Chem.* **2021**, *32*, 2307–2317. [[CrossRef](#)]
25. Shalash, A.O.; Becker, L.; Yang, J.; Giacomini, P.; Pearson, M.; Hussein, W.M.; Loukas, A.; Toth, I.; Skwarczynski, M. Development of a peptide vaccine against hookworm infection: Immunogenicity, efficacy, and immune correlates of protection. *J. Allergy Clin. Immunol.* **2022**, *150*, 157–169.e110. [[CrossRef](#)] [[PubMed](#)]
26. Shalash, A.O.; Becker, L.; Yang, J.; Giacomini, P.; Pearson, M.; Hussein, W.M.; Loukas, A.; Skwarczynski, M.; Toth, I. Oral Peptide Vaccine against Hookworm Infection: Correlation of Antibody Titers with Protective Efficacy. *Vaccines* **2021**, *9*, 1034. [[CrossRef](#)]
27. Bartlett, S.; Skwarczynski, M.; Xie, X.; Toth, I.; Loukas, A.; Eichenberger, R.M. Development of natural and unnatural amino acid delivery systems against hookworm infection. *Precis. Nanomed.* **2020**, *3*, 471–482. [[CrossRef](#)]
28. Ahmad Fuaad, A.A.H.; Skwarczynski, M.; Toth, I. The use of microwave-assisted solid-phase peptide synthesis and click chemistry for the synthesis of vaccine candidates against hookworm infection. *Methods Mol. Biol.* **2016**, *1403*, 639–653.
29. Hussein, W.M.; Cheong, Y.S.; Liu, C.; Liu, G.; Begum, A.A.; Attallah, M.A.; Moyle, P.M.; Torchilin, V.; Smith, R.; Toth, I. Peptide-based targeted polymeric nanoparticles for siRNA delivery. *Nanotechnology* **2019**, *30*, 415604. [[CrossRef](#)]
30. Hussein, W.M.; Toth, I.; Skwarczynski, M. Peptide-Polymer Conjugation Via Copper-Catalyzed Alkyne-Azide 1,3-Dipolar Cycloaddition. In *Peptide Conjugation: Methods and Protocols*; Hussein, W.M., Stephenson, R.J., Toth, I., Eds.; Springer: New York, NY, USA, 2021; pp. 1–7.
31. Giddam, A.K.; Reiman, J.M.; Zaman, M.; Skwarczynski, M.; Toth, I.; Good, M.F. A semi-synthetic whole parasite vaccine designed to protect against blood stage malaria. *Acta Biomater.* **2016**, *44*, 295–303. [[CrossRef](#)]
32. Yang, J.; Firdaus, F.; Azuar, A.; Khalil, Z.G.; Marasini, N.; Capon, R.J.; Hussein, W.M.; Toth, I.; Skwarczynski, M. Cell-Penetrating Peptides-Based Liposomal Delivery System Enhanced Immunogenicity of Peptide-Based Vaccine against Group A Streptococcus. *Vaccines* **2021**, *9*, 499. [[CrossRef](#)]
33. Baldin, A.V.; Savvateeva, L.V.; Bazhin, A.V.; Zamyatnin, A.A., Jr. Dendritic Cells in Anticancer Vaccination: Rationale for Ex Vivo Loading or In Vivo Targeting. *Cancers* **2020**, *12*, 590. [[CrossRef](#)]
34. Liu, Y.; Yao, L.; Cao, W.; Liu, Y.; Zhai, W.; Wu, Y.; Wang, B.; Gou, S.; Qin, Y.; Qi, Y.; et al. Dendritic Cell Targeting Peptide-Based Nanovaccines for Enhanced Cancer Immunotherapy. *ACS Appl. Bio Mater.* **2019**, *2*, 1241–1254. [[CrossRef](#)] [[PubMed](#)]
35. Palucka, K.; Banchereau, J. Cancer immunotherapy via dendritic cells. *Nat. Rev. Cancer* **2012**, *12*, 265–277. [[CrossRef](#)]
36. Curiel, T.J.; Morris, C.; Brumlik, M.; Landry, S.J.; Finstad, K.; Nelson, A.; Joshi, V.; Hawkins, C.; Alarez, X.; Lackner, A.; et al. Peptides identified through phage display direct immunogenic antigen to dendritic cells. *J. Immunol.* **2004**, *172*, 7425–7431. [[CrossRef](#)] [[PubMed](#)]
37. Golani-Armon, A.; Golan, M.; Shamay, Y.; Raviv, L.; David, A. DC3-Decorated Polyplexes for Targeted Gene Delivery into Dendritic Cells. *Bioconjugate Chem.* **2015**, *26*, 213–224. [[CrossRef](#)]
38. Bobrysheva, I.V. Immunomodulator Imunofan Affects Cell Profile of Morphofunctional Zones of Rat Thymus and Delays Its Age-Related Involution. *Bull. Russ. State Med. Univ.* **2016**, 34–38. [[CrossRef](#)]
39. Vinnitsky, L.; Bunatian, K.; Mironova, E.; Akopdjanova, E.; Komarov, A. Immunomodulator imunofan in treatment of post-traumatic complications. *Immunology* **1996**, *89*, li366.
40. Toda, S.; Ishii, N.; Okada, E.; Kusakabe, K.I.; Arai, H.; Hamajima, K.; Gorai, I.; Nishioka, K.; Okuda, K. HIV-1-specific cell-mediated immune responses induced by DNA vaccination were enhanced by mannan-coated liposomes and inhibited by anti-interferon-gamma antibody. *Immunology* **1997**, *92*, 111–117. [[CrossRef](#)]
41. Kojima, N.; Ishii, M.; Kawachi, Y.; Takagi, H. Oligomannose-Coated Liposome as a Novel Adjuvant for the Induction of Cellular Immune Responses to Control Disease Status. *Biomed Res. Int.* **2013**, *2013*, 562924. [[CrossRef](#)]

42. Gu, X.G.; Schmitt, M.; Hiasa, A.; Nagata, Y.; Ikeda, H.; Sasaki, Y.; Akiyoshi, K.; Sunamoto, J.; Nakamura, H.; Kuribayashi, K.; et al. A novel hydrophobized polysaccharide/oncoprotein complex vaccine induces in vitro and in vivo cellular and humoral immune responses against HER2-expressing murine sarcomas. *Cancer Res.* **1998**, *58*, 3385–3390. [[PubMed](#)]
43. Wang, F.; Xiao, W.; Elbahnasawy, M.A.; Bao, X.; Zheng, Q.; Gong, L.; Zhou, Y.; Yang, S.; Fang, A.; Farag, M.M.S.; et al. Optimization of the Linker Length of Mannose-Cholesterol Conjugates for Enhanced mRNA Delivery to Dendritic Cells by Liposomes. *Front. Pharmacol.* **2018**, *9*, 980. [[CrossRef](#)] [[PubMed](#)]
44. Jeong, H.S.; Na, K.S.; Hwang, H.; Oh, P.S.; Kim, D.H.; Lim, S.T.; Sohn, M.H.; Jeong, H.J. Effect of space length of mannose ligand on uptake of mannose-liposome in RAW 264.7 cells: In vitro and in vivo studies. *J. Biomed. Mater. Res. Part A* **2014**, *102*, 4545–4553. [[CrossRef](#)]
45. Nahar, U.J.; Toth, I.; Skwarczynski, M. Mannose in vaccine delivery. *J. Control. Release* **2022**, *351*, 284–300. [[CrossRef](#)]
46. Sedaghat, B.; Stephenson, R.J.; Giddam, A.K.; Eskandari, S.; Apte, S.H.; Pattinson, D.J.; Doolan, D.L.; Toth, I. Synthesis of Mannosylated Lipopeptides with Receptor Targeting Properties. *Bioconjugate Chem.* **2016**, *27*, 533–548. [[CrossRef](#)] [[PubMed](#)]
47. Stanistic, D.I.; Ho, M.-F.; Nevagi, R.; Cooper, E.; Walton, M.; Islam, M.T.; Hussein, W.M.; Skwarczynski, M.; Toth, I.; Good, M.F. Development and Evaluation of a Cryopreserved Whole-Parasite Vaccine in a Rodent Model of Blood-Stage Malaria. *mBio* **2021**, *12*, e0265721. [[CrossRef](#)]
48. Al-Nazal, H.A.; Cooper, E.; Ho, M.F.; Eskandari, S.; Majam, V.; Giddam, A.K.; Hussein, W.M.; Islam, M.T.; Skwarczynski, M.; Toth, I.; et al. Pre-clinical evaluation of a whole-parasite vaccine to control human babesiosis. *Cell Host Microbe* **2021**, *29*, 894–903. [[CrossRef](#)]
49. Ssemaganda, A.; Giddam, A.K.; Zaman, M.; Skwarczynski, M.; Toth, I.; Stanistic, D.I.; Good, M.F. Induction of Plasmodium-Specific Immune Responses Using Liposome-Based Vaccines. *Front. Immunol.* **2019**, *10*, 135. [[CrossRef](#)]
50. Yang, J.R.; Luo, Y.C.; Shibu, M.A.; Toth, I.; Skwarczynski, M. Cell-Penetrating Peptides: Efficient Vectors for Vaccine Delivery. *Curr. Drug Deliv.* **2019**, *16*, 430–443. [[CrossRef](#)] [[PubMed](#)]
51. Skwarczynski, M.; Zaman, M.; Urbani, C.N.; Lin, I.C.; Jia, Z.; Batzloff, M.R.; Good, M.F.; Monteiro, M.J.; Toth, I. Polyacrylate dendrimer nanoparticles: A self-adjuncting vaccine delivery system. *Angew. Chem. Int. Ed.* **2010**, *49*, 5742–5745. [[CrossRef](#)]
52. Zaman, M.; Skwarczynski, M.; Malcolm, J.M.; Urbani, C.N.; Jia, Z.F.; Batzloff, M.R.; Good, M.F.; Monteiro, M.J.; Toth, I. Self-adjuncting polyacrylic nanoparticulate delivery system for group A streptococcus (GAS) vaccine. *Nanomed. Nanotechnol. Biol. Med.* **2011**, *7*, 168–173. [[CrossRef](#)]
53. Guo, Y.; Sakonsiri, C.; Nehlmeier, I.; Fascione, M.A.; Zhang, H.; Wang, W.; Pöhlmann, S.; Turnbull, W.B.; Zhou, D. Compact, Polyvalent Mannose Quantum Dots as Sensitive, Ratiometric FRET Probes for Multivalent Protein–Ligand Interactions. *Angew. Chem. Int. Ed.* **2016**, *55*, 4738–4742. [[CrossRef](#)]
54. Yang, J.; Azuar, A.; Toth, I.; Skwarczynski, M. Liposomes for the Delivery of Lipopeptide Vaccines. In *Vaccine Design: Methods and Protocols, Volume 3. Resources for Vaccine Development*; Thomas, S., Ed.; Springer: New York, NY, USA, 2022; pp. 295–307.
55. Facciola, A.; Visalli, G.; Lagana, P.; La Fauci, V.; Squeri, R.; Pellicano, G.F.; Nunnari, G.; Trovato, M.; Di Pietro, A. The new era of vaccines: The “nanovaccinology”. *Eur. Rev. Med. Pharmacol. Sci.* **2019**, *23*, 7163–7182. [[CrossRef](#)] [[PubMed](#)]
56. Lu, L.; Duong, V.T.; Shalash, A.O.; Skwarczynski, M.; Toth, I. Chemical Conjugation Strategies for the Development of Protein-Based Subunit Nanovaccines. *Vaccines* **2021**, *9*, 563. [[CrossRef](#)]
57. Skwarczynski, M.; Toth, I. Recent advances in peptide-based subunit nanovaccines. *Nanomedicine* **2014**, *9*, 2657–2669. [[CrossRef](#)] [[PubMed](#)]
58. Ghaffar, K.A.; Giddam, A.K.; Zaman, M.; Skwarczynski, M.; Toth, I. Liposomes as nanovaccine delivery systems. *Curr. Top. Med. Chem.* **2014**, *14*, 1194–1208. [[CrossRef](#)] [[PubMed](#)]
59. Song, Y.; Su, Q.; Song, H.; Shi, X.; Li, M.; Song, N.; Lou, S.; Wang, W.; Yu, Z. Precisely Shaped Self-Adjuvanting Peptide Vaccines with Enhanced Immune Responses for HPV-Associated Cancer Therapy. *ACS Appl. Mater. Interfaces* **2021**, *13*, 49737–49753. [[CrossRef](#)] [[PubMed](#)]
60. Liu, Y.; Wu, L.; Tong, R.; Yang, F.; Yin, L.; Li, M.; You, L.; Xue, J.; Lu, Y. PD-1/PD-L1 Inhibitors in Cervical Cancer. *Front. Pharmacol.* **2019**, *10*. [[CrossRef](#)]
61. Domingos-Pereira, S.; Galliverti, G.; Hanahan, D.; Nardelli-Haeffliger, D. Carboplatin/paclitaxel, E7-vaccination and intravaginal CpG as tri-therapy towards efficient regression of genital HPV16 tumors. *J. Immunother. Cancer* **2019**, *7*, 122. [[CrossRef](#)]
62. Kokate, R.A.; Thamake, S.I.; Chaudhary, P.; Mott, B.; Raut, S.; Vishwanatha, J.K.; Jones, H.P. Enhancement of anti-tumor effect of particulate vaccine delivery system by ‘Bacteriomimetic’ CpG functionalization of poly-lactic-co-glycolic acid nanoparticles. *Nanomedicine* **2015**, *10*, 915–929. [[CrossRef](#)]
63. Liu, C.; Chu, X.; Sun, P.; Feng, X.; Huang, W.; Liu, H.; Ma, Y. Synergy effects of Polyinosinic-polycytidylic acid, CpG oligodeoxynucleotide, and cationic peptides to adjuvant HPV E7 epitope vaccine through preventive and therapeutic immunization in a TC-1 grafted mouse model. *Hum. Vaccines Immunother.* **2018**, *14*, 931–940. [[CrossRef](#)]
64. Kim, T.G.; Kim, C.H.; Won, E.H.; Bae, S.M.; Ahn, W.S.; Park, J.B.; Sin, J.I. CpG-ODN-stimulated dendritic cells act as a potent adjuvant for E7 protein delivery to induce antigen-specific antitumor immunity in a HPV 16 E7-associated animal tumour model. *Immunology* **2004**, *112*, 117–125. [[CrossRef](#)] [[PubMed](#)]
65. Da Silva, D.M.; Skeate, J.G.; Chavez-Juan, E.; Lühen, K.P.; Wu, J.-M.; Wu, C.-M.; Kast, W.M.; Hwang, K. Therapeutic efficacy of a human papillomavirus type 16 E7 bacterial exotoxin fusion protein adjuvanted with CpG or GPI-0100 in a preclinical mouse model for HPV-associated disease. *Vaccine* **2019**, *37*, 2915–2924. [[CrossRef](#)] [[PubMed](#)]

66. Rad-Malekshahi, M.; Fransen, M.F.; Krawczyk, M.; Mansourian, M.; Bourajjaj, M.; Chen, J.; Ossendorp, F.; Hennink, W.E.; Mastrobattista, E.; Amidi, M. Self-Assembling Peptide Epitopes as Novel Platform for Anticancer Vaccination. *Mol. Pharm.* **2017**, *14*, 1482–1493. [[CrossRef](#)]
67. Rahimian, S.; Fransen, M.F.; Kleinovink, J.W.; Christensen, J.R.; Amidi, M.; Hennink, W.E.; Ossendorp, F. Polymeric nanoparticles for co-delivery of synthetic long peptide antigen and poly IC as therapeutic cancer vaccine formulation. *J. Control. Release* **2015**, *203*, 16–22. [[CrossRef](#)] [[PubMed](#)]
68. Zwaveling, S.; Ferreira Mota, S.C.; Nouta, J.; Johnson, M.; Lipford, G.B.; Offringa, R.; van der Burg, S.H.; Melief, C.J. Established human papillomavirus type 16-expressing tumors are effectively eradicated following vaccination with long peptides. *J. Immunol.* **2002**, *169*, 350–358. [[CrossRef](#)] [[PubMed](#)]
69. De Oliveira, L.M.; Morale, M.G.; Chaves, A.A.; Cavalher, A.M.; Lopes, A.S.; Diniz Mde, O.; Schanoski, A.S.; de Melo, R.L.; Ferreira, L.C.; de Oliveira, M.L.; et al. Design, Immune Responses and Anti-Tumor Potential of an HPV16 E6E7 Multi-Epitope Vaccine. *PLoS ONE* **2015**, *10*, e0138686. [[CrossRef](#)]
70. Nguyen, C.T.; Hong, S.H.; Sin, J.-I.; Vu, H.V.D.; Jeong, K.; Cho, K.O.; Uematsu, S.; Akira, S.; Lee, S.E.; Rhee, J.H. Flagellin enhances tumor-specific CD8+ T cell immune responses through TLR5 stimulation in a therapeutic cancer vaccine model. *Vaccine* **2013**, *31*, 3879–3887. [[CrossRef](#)]
71. Namvar, A.; Panahi, H.A.; Agi, E.; Bolhassani, A. Development of HPV(16,18,31,45) E5 and E7 peptides-based vaccines predicted by immunoinformatics tools. *Biotechnol. Lett.* **2020**, *42*, 403–418. [[CrossRef](#)]
72. Gan, L.; Jia, R.; Zhou, L.; Guo, J.; Fan, M. Fusion of CTLA-4 with HPV16 E7 and E6 enhanced the potency of therapeutic HPV DNA vaccine. *PLoS ONE* **2014**, *9*, e108892. [[CrossRef](#)]
73. Peng, S.; Tan, M.; Li, Y.D.; Cheng, M.A.; Farmer, E.; Ferrall, L.; Gaillard, S.; Roden, R.B.S.; Hung, C.F.; Wu, T.C. PD-1 blockade synergizes with intratumoral vaccination of a therapeutic HPV protein vaccine and elicits regression of tumor in a preclinical model. *Cancer Immunol. Immunother.* **2021**, *70*, 1049–1062. [[CrossRef](#)]

Disclaimer/Publisher’s Note: The statements, opinions and data contained in all publications are solely those of the individual author(s) and contributor(s) and not of MDPI and/or the editor(s). MDPI and/or the editor(s) disclaim responsibility for any injury to people or property resulting from any ideas, methods, instructions or products referred to in the content.